Chronological age, changes in DNA methylation, and endogenous hormone levels of explants promote somatic embryogenesis of Euterpe edulis Martius

Tamyris de Mello

tamyrisdemello@gmail.com

Universidade Federal do Espirito Santo https://orcid.org/0000-0003-1189-5404

TadeuÉriton Caliman Zanardo

UFES: Universidade Federal do Espirito Santo

Tatiane Dulcineia Silva

UFV: Universidade Federal de Vicosa

Joana Silva Costa

UFES: Universidade Federal do Espirito Santo

Débora Pellanda Fagundes

UFES: Universidade Federal do Espirito Santo

Caroline Palacio de Araujo

UFES: Universidade Federal do Espirito Santo

Clovis Eduardo Nunes Hegedus

UFES: Universidade Federal do Espirito Santo

Breno Benvindo dos Anjos

UFES: Universidade Federal do Espirito Santo

Edilson Romais Schmildt

UFES: Universidade Federal do Espirito Santo

Adésio Ferreira Ferreira

UFES: Universidade Federal do Espirito Santo

Márcia Flores da Silva Ferreira

UFES: Universidade Federal do Espirito Santo

José Carlos Lopes

UFES: Universidade Federal do Espirito Santo

Wagner Campos Otoni

UFV: Universidade Federal de Vicosa

Rodrigo Sobreira Alexandre

UFES: Universidade Federal do Espirito Santo

Research Article

Keywords: juçara, in vitro, explant maturity, picloram, DNA methylation, polyamines

Posted Date: December 29th, 2023

DOI: https://doi.org/10.21203/rs.3.rs-3756044/v1

Version of Record: A version of this preprint was published at Plant Cell, Tissue and Organ Culture (PCTOC) on April 25th, 2024. See the published version at https://doi.org/10.1007/s11240-024-02757-x.

Abstract

Euterpe edulis Martius is an endangered palm tree native to the Atlantic Forest. As it propagates only with seeds and does not tiller, the tree dies after its highly appreciated palm heart is harvested. In this study, we analyzed the embryogenic response of *E. edulis* with respect to maturity of the explant and concentration of picloram, an auxin mimetic. Immature fruits were harvested, and their seeds were extracted and germinated *in vitro*. After 2, 4, 6, and 8 months, the aerial parts of normal seedlings were excised and stem segments were used to induce somatic embryogenesis in the presence of 100, 125, 150, 175, and 200 μM picloram. The number of proembryos, induction rate, explant mass, oxidation, global DNA methylation, 1-aminocyclopropane-1-carboxylic acid, proline, polyamines, and ultrastructural analysis of cells were assessed. Six-month-old seedling explants achieved the highest number of proembryos and embryogenic induction rate at most picloram concentrations, as well as the highest 1-aminocyclopropane-1-carboxylic acid content, but lowest spermine and putrescine levels. Explants with somatic embryos exhibited lower DNA methylation levels than non-embryogenic calli. Proline content was highest in stem segments of younger seedlings (2-month-old). Despite being asynchronous, maturation with 5 μM abscisic acid was achieved. Therefore, 6-month-old *E. edulis* seedlings supplemented with 200 μM picloram could be used for *ex situ* conservation of this endangered species.

1 INTRODUCTION

Euterpe edulis Martius is a palm tree native to the Atlantic Forest and currently threatened with extinction due to overharvesting. Its palm heart is considered a culinary delicacy but, because the plant is single-stemmed and does not tiller, it dies after the heart has been removed (Schulz et al. 2016). Recently, the global craze for açaí berries has opened a more sustainable form of exploitation of *E. edulis*. Its fruits are sweeter and have superior nutritional properties compared to açaí berries obtained from *Euterpe oleracea* Martius and *Euterpe precatoria* Martius (Borges et al. 2013), making *E. edulis* relevant from both a conservation and an economic point of view (Garcia et al. 2019).

Propagation of this species takes place solely by seeds, which are produced annually and whose collection is hampered by the height of the tree (5–12 m), as well as by wide animal-based dispersion (Schulz et al. 2016). Lack of tillering limits asexual reproduction and imposes a barrier to large-scale propagation.

Somatic embryogenesis is the most efficient biotechnological tool for the propagation of certain plants (Corredoira et al. 2019). However, somatic cells become competent and acquire embryogenic potential only upon stimulation. The latter often depends on dedifferentiation, the activation of cell division to maintain a new destiny, and embryo induction (Isah 2016).

The ability of somatic cells from an explant to become embryogenic decreases with increasing age of the parent plant, possibly because of a reduced response to growth regulators (Ikeuchi et al. 2016). Therefore, the maturity of parental tissues can influence embryogenic responses by affecting the ability

to transport growth regulators and have them bind to the induction genes, as well as the metabolic capacity of cells (Isah 2016).

Growth regulators act as signaling molecules, and can promote modifications in chromatin domains such as DNA methylation, thereby altering gene expression patterns (Rodríguez-Sanz et al. 2014; Silva-Cardoso et al. 2022). These epigenetic modifications have been reported during the induction of embryogenesis in at least 18 species from 12 botanical families (De-La-Peña et al. 2015).

Generally, embryogenic tissues exhibit lower DNA methylation levels than non-embryogenic tissues, suggesting that hypomethylation is a prerequisite for successful induction of somatic embryogenesis (De-La-Peña et al. 2015). Somatic embryogenesis of *Elaeis oleifera* × *Elaeis guineenses* hybrids revealed that the formation of calli was related to DNA hypomethylation in the B351733 hybrid; whereas the non-responsiveness of leaf explants was related to DNA hypermethylation in the B352932 hybrids (Silva-Cardoso et al. 2022). In the same atudy, the first macroscopic anatomical changes associated with callus formation were reported after 90 days of culture, coinciding with the occurrence of DNA hypomethylation. Hence, DNA methylation may be a good embryogenic indicator.

The choice of explant for subsequent embryogenic induction requires detailed knowledge of how the starting material may respond to culture conditions. Therefore, the objective of this study was to analyze the embryogenic response of *E. edulis* in relation to the maturity of the explants and the concentration of picloram. We report that the age of explant donor plants associated with lower levels of DNA methylation, while picloram favored cellular competence. These findings describe a reliable approach for *ex situ* conservation of this iconic yet threatened species.

2 MATERIAL AND METHODS

2.1 Collection, disinfection, and establishment

The fruits of *E. edulis* were harvested from a mother plant with height of 6.7 m and diameter at breast height (1.3 m) of 13.4 cm, located in the district of Pedra Menina, in the municipality of Dores do Rio Preto, Espírito Santo, Brazil. The location was near Caparaó National Park, at 20º32'45.4" S, 41º49'35.7" W, and an altitude of 951 m. The fruits were harvested approximately 168 days after anthesis, and were sent to the Laboratory of Forest Seeds and Plant Tissue Culture at the Center for Agricultural Sciences and Engineering, Federal University of Espírito Santo, where fresh and dry mass (g), seed water content (%), mean fruit diameter (mm), and volume (cm^3) were recorded.

After cleaning the fruits, the seed coat was removed and the seeds were immersed in 2% ascorbic acid to prevent phenolic oxidation. In a laminar flow chamber, *E. edulis* seeds were immersed in 70% ethyl alcohol for 60 s, 2.5% sodium hypochlorite (Candura) for 10 min, and 3 g L^{-1} amoxicillin (Germed) for 10 min, followed by triple washing in distilled and autoclaved water after each step.

The seeds were arranged in test tubes (25 × 150 mm) containing 10 mL MS culture medium (Murashige and Skoog 1962) (Sigma), supplemented with 1 g L^{-1} polyvinylpyrrolidone (Synth), 30 g L^{-1} sucrose (Dinâmica), 0.1 g L^{-1} myoinositol (Sigma), and 5.5 g L^{-1} agar (Kasvi). The pH of the medium was adjusted to 5.7 ± 0.1 with 1 N KOH (Alphatec) and/or 1 N HCl (Vetec). Test tubes were capped with 25-mm polypropyline caps (Sigma) before autoclaving at 121°C and 15 psi for 15 min.

The explants were kept in a growth room at a 27 ± 2°C in the dark until seedlings were obtained after 2, 4, 6, and 8 months. During this period, data on germination percentage (%) (Brasil 2009), relative frequency of germination, germination speed index (Maguire 1962), and average germination time (days) (Labouriau 1983) were collected. Seedling height (cm), stem diameter (mm), and fresh and dry shoot mass (g) were evaluated at each age.

2.2 Induction

Seedlings of each age were excised at the collar and apex, leaving the middle part of approximately 20 mm. This was sectioned first transversely into two 10-mm explants and then longitudinally. The explants were arranged with the wound surface facing upward in MS culture medium with 0.1 g L^{-1} myo-inositol, 1 g L^{-1} polyvinylpyrrolidone, and 30 g L^{-1} sucrose. The pH was adjusted to 5.7 ± 0.1 before adding 5.5 g L^{-1} agar. After autoclaving, the medium was supplemented with 100, 125, 150, 175, and 200 µM filtered 4-amino-3,5,6-trichloro-2-pyridinecarboxylic acid (picloram).

The experiments were performed in a growth room at 27 ± 2°C in the dark for 60 days. The number of proembryos, induction rate (%), explant mass (g), and oxidation (%) were analyzed.

Histological and structural analyses

For anatomical studies, the samples were dehydrated in an ethyl series and soaked in methacrylate (Historesin®, Leica). Transversal and longitudinal sections (5-µm-thick) were obtained with an automatic rotating microtome (RM2155, Leica) equipped with a disposable glass razor, and stained with toluidine blue at pH 4.0 for 15 min (O'Brien and McCully 1981). The slides were mounted in synthetic resin (Permount®, Fisher Scientific) and observed under a light microscope (Olympus-AX 70) coupled with a photomicrography system (Olympus U-Photo) at the Laboratory of Plant Anatomy, Department of Plant Biology, Federal University of Viçosa.

Genomic DNA extraction

Briefly, 200 mg of embryogenic and non-embryogenic samples of *E. edulis* cultivated *in vitro* were used. They were first macerated with liquid nitrogen and then dissolved in extraction buffer containing 100 mM Tris-HCl pH 8.0, 2% (w w^{-1}) cetyl trimethyl ammonium bromide, 1.4 M NaCl, 20 mM EDTA pH 8.0, 0.2% (w v^{-1}) β-mercaptoethanol, and 0.1 mg mL^{-1} proteinase K. After incubation for 30 min at 65°C, 650 µL of CIA solution containing 96% (v v^{-1}) chloroform and 4% (v v^{-1}) isoamyl alcohol was added, and the samples were homogenized and centrifuged at 12000 rpm for 10 min. The resulting aqueous phase was

transferred to clean microtubes, another 650 µL of CIA solution was added, and the samples were centrifuged again at 12000 rpm for 10 min.

DNA was precipitated by adding one volume of isopropanol at 4°C, after which aliquots were centrifuged at 12000 rpm for 15 min. The supernatant was discarded and the precipitate was washed twice with 70% ethanol. The pellet was dried in a Vacufuge® Plus concentrator (Eppendorf) for 10 min. At the end of the extraction, the samples were resuspended in 40 µL TE solution (10 mM Tris-HCl pH 8.0, 1 mM EDTA pH 8.0, 40 µg mL^{-1} RNAse) and incubated at 37°C for 30 min to degrade any residual RNA.

Determination of global methylation content

Briefly, 30 µg of DNA was used per sample of biological material. The DNA sample was dissolved in 100 µL ultrapure water and 50 µL perchloric acid (70% v v^{-1}), and then heated at 100°C for 60 min. Subsequently, the pH was adjusted to 3–5 by adding 1 M KOH, and the samples were centrifuged at 10000 rpm for 5 min. The supernatant was transferred to a new microtube, and 200 µL ultrapure water was added to elute twice the DNA remaining in the precipitate. The microtubes were centrifuged at 10000 rpm for 5 min and the supernatant was transferred to a new tube, which was then dried in a Vacufuge® Plus concentrator under vacuum for 5 h.

The samples were resuspended in 100 µL ultrapure water, centrifuged at 10000 rpm for 5 min, transferred to vials containing inserts, and analyzed in a high-performance liquid chromatographer equipped with a Zorbax Eclipse XDB-C18 stainless steel column (4.6 × 250 mm, 5 µm particle size; Agilent) at a monitored wavelength of 270 nm and flow rate of 0.5 mL min^{-1}.

To determine the amount of methylated cytosine in the samples, the percentage of 5-methylcytosine (5mC) in DNA was calculated according to the following equation: 5mC (%) = (A5mC / A5mc + AC) × 100, where A5mC is the peak area of 5mC and AC is the peak area of cytosine.

Transmission electron microscopy

Samples from different experimental groups were collected and fixed in Karnovsky's solution containing 2.5% glutaraldehyde, 2% paraformaldehyde, and 0.1 M cacodylate buffer. Subsequently, the tissues were post-fixed in osmium tetroxide, dehydrated in ethanol (30%, 50%, 70%, 90%, and 100%), and embedded in epoxy resin (EMbed 812, Eletron Microscopy Sciences). Ultrathin sections (60–80 nm in thickness) were obtained using an ultramicrotome (UCT, Leica Microsystems) before staining with uranyl acetate and lead citrate. Representative micrographs were obtained using a transmission electron microscope (JEOL JEM-1400) at 120 kV and 12000x magnification. Analysis was performed at the Laboratory of Cellular Ultrastructure Carlos Alberto Redins, Federal University of Espírito Santo.

Determination of 1-aminocyclopropane-1-carboxylic acid, proline, and polyamines

Extraction of the ethylene precursor 1-aminocyclopropane-1-carboxylic acid (ACC), proline, and polyamines (spermine and spermidine) was carried out using the aerial parts of seedlings (2, 4, 6, and 8 months) and the respective embryogenic calli (150 µM picloram) as described by Forcat et al. (2008).

Samples from each treatment were macerated in a crucible with liquid nitrogen and 0.110 g per sample was placed in 2-mL microcentrifuge tubes. Then, 400 µL methanol:isopropanol:acetic acid extraction solution (20:79:1) was added, each sample mixture was vortexed four times for 20 s, and finally sonicated for 10 min. The samples were allowed to rest for 30 min on ice, followed by sonication for 10 min and centrifugation at 13000 rpm for 10 min at 4°C. The supernatant was collected, mixed with 400 µL extraction solution, and all steps were repeated again. Subsequently, the samples were filtered through 13-mm and 0.22-µm polyvinylidene fluoride syringe filters.

Quantification was performed by injecting 300 µL of the sample extract in an ultra-high-performance liquid chromatographer coupled to a triple quadrupole mass spectrometer. Skyline Software was used to obtain the peak areas and ACC mass, which was calculated using the equation: $Y = 289.81X + 7.5177$, $R^2 = 0.9995$. The final result was expressed in ng g^{-1}. Proline and polyamines were analyzed for relative abundance using the equation: AR (%) = (callus treatment area / seedling treatment area) × 100.

Experimental design

The design was completely randomized in a 4 × 5 factorial, consisting of age (2, 4, 6, and 8 months) × picloram concentrations (100, 125, 150, 175, and 200 µM). Ten replications with four explants, and triplicates for ACC, proline, and polyamines were included. Data were subjected to analysis of variance and Tukey's test ($p < 0.05$) (R Core Team 2020).

2.3 Maturation

Explants containing somatic embryos were transferred to MS culture medium supplemented with 0.1 g L^{-1} myo-inositol, 1 g L^{-1} polyvinylpyrrolidone, and 30 g L^{-1} sucrose. The pH of the medium was adjusted to 5.7 ± 0.1 prior to addition of 5.5 g L^{-1} agar and 5 µM abscisic acid (Sigma). The experiment was conducted in a growth room at 27 ± 2°C in the dark for 60 days.

2.4 Conversion of emblings and acclimatization

After maturation, somatic embryos were transferred to MS culture medium, supplemented with 0.1 g L^{-1} myo-inositol, 1 g L^{-1} PVP, and 30 g L^{-1} sucrose. The pH of the medium was adjusted to 5.7 ± 0.1 prior to the addition of agar (5.5 g L^{-1}).

After that period (30 days), they were placed in an *ex-vitro* environment consisting of plastic cups (590 mL) containing autoclaved substrate (TerraNutri®) moistened with distilled and autoclaved water. Each cup was covered with another cup (300 mL) to maintain the humidity during the first 7 days. Following that period, two holes (Θ = 0.5 cm) were made in the upper cup every 2 days, and the cultures were incubated for another 10 days (Mello et al. 2023).

3 RESULTS

3.1 Induction

Immature seeds (~ 180 days after anthesis) weighted on average 1.69 g (fresh mass), had a moisture content of 67.36%, and displayed 100% germination *in vitro*, with an average germination speed index of 2.20 and germination time of 11.71 days (Fig. 1a). Post-germination growth of seedlings followed a linear trajectory (Fig. 1b).

Six-month-old seedlings presented the highest average proembryo number and embryogenic induction rate at most picloram concentrations (100, 125, 150, and 200 μM) (Fig. 2a, b), with 200 μM yielding the highest mean fresh mass (Fig. 2c). Induction in seedlings aged 2 and 4 months was negatively affected by higher tissue oxidation levels (Fig. 2d). Overall, embryogenic induction of *E. edulis* seedlings appeared to show a slight decline after 6 months.

The formation of somatic embryos occurred directly and asynchronously after 60 days of induction, with embryos of different shapes, colors, and sizes being observed (Fig. 3). They were visibly more abundant in explants from 6-month-old seedlings (Fig. 3c and Fig. 4a).

In addition to somatic embryos on the explant surface, clusters of cells forming proembryos within the explant tissue and emerging cells could be observed in histological sections (Fig. 4b, c). Somatic embryos were formed at the globular stage from a unicellular origin (with suspensor) and a multicellular origin directly from meristematic cells (Fig. 4d, e).

In histological sections, heavily stained layers of meristematic cells were detected. These regions differed from others based on clusters of small isodiametric cells with dense cytoplasm and conspicuous nuclei. It was also possible to observe subepidermal cells dividing in different planes, forming clusters of cells in anticlinal and periclinal divisions. These meristematic zones presented heavily stained regions, which indicated intense cell division, as well as a defined protoderm (Fig. 4f).

During induction, both embryogenic structures containing somatic embryos, as well as non-embryogenic structures were detected (Fig. 5a–f). Overall DNA methylation was lower in embryogenic samples with somatic embryos (31–45%) than in non-embryogenic samples (74–99%) (Fig. 5g).

The difference between seedling age became clear when analyzing embryogenic tissue at the cellular level (Fig. 6). Explants induced from 2-month-old seedlings had more fragmented vacuoles and more evident amyloplasts, with prominent starch granules, compared to those induced from 8-month-old seedlings (Fig. 6a, d, g, j). Other embryogenic characteristics were common to both explant types, including a dense cytoplasm; evident nuclei and nucleoli; large, electron-dense, and irregularly shaped nuclei; lower heterochromatin to euchromatin content (Fig. 6a, b, g, h); numerous mitochondria and a prominent endoplasmic reticulum and Golgi complex, a (Fig. 6c, e, j, k) closely attached to the cell wall; and thick cell walls (Fig. 6f, l).

The concentration of ACC increased after induction for most seedlings, except 2-month-old ones, wheereby it decreased from 42.5 to 12.5 ng g^{-1}. The shoots of 6-month-old seedlings contained the lowest concentration of ACC (34.1 ng g^{-1}) with respect to seedling age but the highest concentration among calli (94.5 ng g^{-1}) (Fig. 7a).

Embryos obtained from 2-month-old seedlings presented the highest proline content (75%) (Fig. 7b). Spermine and spermidine attained the largest concentrations in embryos derived from 4-month-old seedlings (Fig. 7c, d). The lowest spermine content was detected in 6- and 8-month-old seedlings (Fig. 7c); whereas putrescine was lowest in 6-month-old seedlings (Fig. 7e).

3.2 Maturation

After 60 days of maturation, the explants showed asynchronous growth, as indicated by the presence of somatic embryos at different stages of development (Fig. 8a), including globular stage with suspensor (Fig. 8b), embryos in transition between stages (Fig. 8c), and scutellar and coleoptilar embryos (Fig. 8d, e).

3.3 Conversion of emblings and acclimatisation

Embryos at the coleoptilary stage grew well in embling conversion medium (Fig. 9a), becoming ready to germinate.

Germinated embryos showed reddish tissue at the tip of the primary root (Fig. 9b), and whitish shoots (Fig. 9c). Once formed, normal emblings (Fig. 9d) remained green throughout the acclimatisation process (Fig. 9e).

4 DISCUSSION

Six-month-old *E. edulis* seedlings showed adequate vertical and radial growth, and are therefore indicated for stem extraction and subsequent embryogenic induction with picloram (200 µM).

Competence is acquired by adapting to the stress derived from *in vitro* cultivation. It results in reprogramming of gene expression and cell division patterns, and leads to changes in cell fate (Fehér 2005). In general, competent cells exhibit meristematic characteristics during the induction phase, such as small size, isodiametric shape, dense cytoplasm, as well as prominent nuclei and nucleoli (Fig. 4).

Somatic embryos can differentiate directly from explants, forming primary centers and subsequent proembryos. This phase is marked by intense mitotic activity, RNA synthesis, and metabolic activity (Oliveira et al. 2022). Another structure that can be observed at the beginning of somatic embryo formation is the suspensor, which points to the unicellular origin of somatic embryos (Ferreira et al. 2022). The visualization of structures similar to suspensors during somatic embryogenesis has already been reported in this species (Guerra and Handro 1998) and in other palm trees of the same genus, such as *E. oleracea* (Scherwinski-Pereira et al. 2012; Freitas et al. 2016)d *precatoria* (Ferreira et al. 2022).

Here, we observed also embryos of multicellular origin, which seemed to merge with the tissue of origin, as well as the fusion of somatic embryos (Fig. 4e, f).

Tissue culture-induced molecular and phenotypic changes arise from stress conditions and continuous subculture in an *in vitro* environment. They often lead to epigenetic variations such as altered DNA methylation patterns (Ghosh et al. 2021). In the present study, non-embryogenic calli were characterized by DNA hypermethylation (> 74–99%); whereas embryogenic calli displayed lower %5mC values (31%) (Fig. 5).

In a study of *Coffea canephora* Pierre ex Froehner, the stages of competence acquisition, determination, and cell differentiation were marked by increases in %5mC (38.4%), abscisic acid, and indole-3-acetic acid, along with decreases in ACC and spermidine, indicating that these changes triggered regeneration and maturation of somatic embryos (Amaral-Silva et al. 2021).

Overall DNA methylation content varies widely across species, organs, and developmental stages. Demethylation in a specific cell mass or organ occurs before the initiation of any differentiation program such as somatic embryogenesis. Instead, DNA hypermethylation may occur during tissue aging, along with the loss of morphogenetic competence (Valledor et al. 2007).

Some studies on woody species have shown that low levels of DNA methylation are associated with morphogenic and embryogenic capabilities. Specifically, DNA methylation appears to be lower in embryogenic masses and early embryos compared with non-embryogenic cells (Chakrabarty et al. 2003; Valledor et al. 2007; Rodriguez-Sanz et al. 2014; Corredoira et al. 2017).

DNA hypomethylation correlates with chromatin decondensation in the early stages of embryogenesis. Hence, embryogenic cell nuclei exhibit a %5mC pattern compatible with a lower heterochromatin to euchromatin content (Fig. 5b, h); whereas the opposite is observed in non-embryogenic cell nuclei. Such chromatin compaction prevents the transcription machinery from accessing the DNA, thereby affecting gene regulation and silencing in heterochromatic regions (Rodriguez-Sanz et al. 2014).

Therefore, the greater embryogenic response of explants from older (6- or 8-month-old) seedlings compared to younger ones (2- or 4-month-old) may be related to a lower heterochromatin to euchromatin content (Fig. 5b, h) of embryogenic cells with somatic embryos (Fig. 4g).

The abundance of organelles observed in embryogenic cells, mainly mitochondria and the endoplasmic reticulum, indicates intense RNA synthesis and high metabolic activity (Stein et al. 2010). The presence of numerous mitochondria is typical of embryogenic systems with elevated metabolic activity arising from high respiratory rates. A well developed endoplasmic reticulum with concentric layers has been observed in other embryogenic systems (Rocha et al. 2016), where it has been associated with strong protein synthesis and transport to other parts of the cell.

Reserve compounds, as the starch observed in the transmission electron microscopy in the present work, are necessary for cell reorganization and differentiation, and they are found in mitotically active

tissues, whereby they provide energy during cell division and successive formation of embryogenic cells and proembryos (Rocha et al. 2016). Starch content decreases with the differentiation of embryogenic areas, leading to fewer starch grains in proembryos and somatic embryos (Silva-Cardoso et al. 2019).

S-adenosyl-1-methionine is converted to ACC by ACC synthase and then to ethylene by ACC oxidase (Yang and Hoffman 1984). Elevated endogenous ACC correlates with high ethylene production. Moreover, both ACC and ethylene are involved in the regulation of embryogenesis *in vivo* and *in vitro* (Kępczyńska at al. 2009).

Ethylene controls somatic embryogenesis in several liliopsida and magnoliopsida species, and a high level of ACC may be a prerequisite for early differentiation during embryogenesis induction (Huang et al. 2008; Kępczyńska et al. 2009). This is based on evidence from explants of *Medicago sativa* petioles, which released ten times more ethylene when maintained in induction compared to differentiation medium. The presence of ethylene in calli grown for 14 days in induction medium can be explained by a large internal pool of ACC, which allows for callus induction and which is regenerated by ACC synthase upon stimulation with exogenous auxins present in the culture medium (Huang et al. 2008).

Amino acids represent an important reserve of organic nitrogen, which is essential for protein synthesis and as precursors of primary and secondary metabolites (Hildebrandt et al. 2015). Proline acts as an osmolyte and chemical chaperone, and accumulates in plants under various stress conditions (Hildebrandt et al. 2015). Here, the explants obtained from the youngest (2-month-old) seedlings were the most subjected to stress caused by embryogenic induction, as confirmed by the highest proline content.

Polyamines also play a crucial modulatory role in growth and development, as well as in response to biotic and abiotic stress. Increased polyamine levels in plant cells are considered part of the stress response mechanism (Nandy et al. 2022). The antioxidant enzymes superoxide dismutase, catalase, peroxidase, monodehydroascorbate reductase, dehydroascorbate reductase, glutathione reductase, glutathione S-transferase, and glutathione peroxidase were found to augment with an increased supply of spermine (Hassan et al., 2021). Putrescine plays a key role during the early rapid cell division stage; whereas spermine and spermidine become important during the rapid cell elongation phase at the end of embryo growth. Therefore, putrescine is responsible for the generation of somatic embryos; while spermidine and spermine promote maturation by regulating different developmental cascades (Nandy et al. 2022; Polesi et al. 2022).

Maturation of *E. edulis* is stimulated by the growth regulators 1-naphthaleneacetic acid (0.53 μM) and 2-isopentenyladenine (12.3 μM) (Guerra and Handro 1998; Oliveira et al. 2022). In the present study, the use of abscisic acid alone (5 μM) was sufficient for maturation. Abscisic acid increases endogenous polyamine (spermine) content (Toumi et al. 2010), stimulates the storage of reserve substances (Gutmann et al. 1996), and induces the final development of the embryo through accumulation of late embryogenesis abundant proteins (Dodeman et al. 1997). Thus, the maturation of asynchronous

embryos is common during somatic embryogenesis in *Euterpe* palms (Guerra and Handro 1988; 1998; Ledo et al. 2002; Scherwinski-Pereira et al. 2012; Freitas et al. 2016; Ferreira et al. 2022).

5 CONCLUSION

In summary, 6-month-old *E. edulis* seedlings appear to be the most suitable source of stem segments and the most responsive to embryogenic induction with picloram (200 μM).

Induced explants exhibited a higher starch content when originating from younger (2-month-old) than from older (8-month-old) seedlings. Stem-derived segments of younger seedlings were most influenced by the stress caused by embryogenic induction, as evidenced by greater proline accumulation. Instead, explants generated from 6-month-old seedlings attained the highest ACC levels but lowest spermine and putrescine content.

Explants with somatic embryos have lower global DNA methylation levels than non-embryogenic calli.

Finally, abscisic acid alone (5 μM) was sufficient for the maturation of somatic embryos of *E. edulis*.

Declarations

Funding

This study was funded by the Fundação de Amparo à Pesquisa e Inovação do Espírito Santo (FAPES) (EDITAL FAPES/CNPq N° 05/2017 - PRONEM - PROGRAMA DE APOIO A NÚCLEOS EMERGENTES). The agreement was registered with SICONV under n° 794009/2013, Process FAPES n° 72660945, and Conselho Nacional de Desenvolvimento Científico e Tecnológico (CNPq) (Finance code 308365/2019-4).

CRediT authorship contribution statement

Tamyris de Mello: Investigation, Methodology, Writing – review and editing. **Tadeu Ériton Caliman Zanardo**, **Tatiane Dulcineia Silva**, **Joana Silva Costa**, **Débora Pellanda Fagundes**, **Caroline Palacio de Araujo**, and **Clovis Eduardo Nunes Hegedus**: Investigation, Writing – review and editing. **Breno Benvindo do Anjos**, **Edilson Romais Schmildt**, and **Adésio Ferreira**: Formal analysis. **Marcia Flores da Silva Ferreira**, **José Carlos Lopes**, and **Wagner Campos Otoni**: Supervision, Writing – original draft, Writing – review and editing. **Rodrigo Sobreira Alexandre**: Conceptualization, Supervision, Project administration, Funding acquisition, Writing – original draft, Writing – review and editing.

Declaration of Competing Interest

The authors have no relevant financial or non-financial interests to disclose.

Acknowledgments

The authors would like to thank Conselho Nacional de Desenvolvimento Científico e Tecnológico (CNPq) and Fundação de Amparo à Pesquisa e Inovação do Espírito Santo (FAPES) for research funding and Editage (www.editage.com) for English language editing. In addition, the authors are grateful to the Carlos Alberto Redins Cellular Ultrastructure Multiuser Laboratory (LUCCAR) on behalf of Prof. Dr. Breno Valentim Nogueira.

Declaration of data availability

The datasets generated during and/or analysed during the current study are available from the corresponding author on reasonable request.

References

1. Amaral-Silva PM, Clarindo WR, Guilhen JHS, Passos ABRJ, Sanglard NA, Ferreira A (2021) Global 5-methylcytosine and physiological changes are triggers of indirect somatic embryogenesis in *Coffea canephora*. Protoplasma 258:45-57. https://doi.org/10.1007/s00709-020-01551-8
2. Borges GSC, Gonzaga LV, Jardini FA, Mancini Filho J, Hellerm MG, Costa ACO, Fett R (2013) Protective effect of *Euterpe edulis* M. on Vero cell culture and antioxidant evaluation based on phenolic composition using HPLC– ESI-MS/MS. Food Rese Int 51(1):363-369. https://doi.org/10.1016/j.foodres.2012.12.035
3. Chakrabarty D, Yuk KW, Paek KY (2003) Detection of DNA methylation changes during somatic embryogenesis of Siberian ginseng (*Eleuterococcus senticosus*). Plant Sci 165(1):61-68. https://doi.org/10.1016/S0168-9452(03)00127-4
4. Corredoira E, Cano V, Bárány I, Solís MT, Rodríguez H, Vieitez AM, Risueño MC, Testillano PS (2017) Initiation of leaf somatic embryogenesis involves high pectin esterification, auxin accumulation and DNA demethylation in *Quercus alba*. J Plant Physiol213:42-54. https://doi.org/10.1016/j.jplph.2017.02.012
5. Corredoira E, Merkle SA, Martínez MT, Toribio M, Canhoto JM, Correia SI, Ballester A, Vieitez AM (2019) Non-zygotic embryogenesis in hardwood species. Crit Rev Plant Sci 38(1)29-97. https://doi.org/10.1080/07352689.2018.1551122
6. De-La-Peña C, Nic-Can GI, Galaz-Ávalos RM, Avilezmontalvo R, Loyola- Argas VM (2015) The role of chromatin modifications in somatic embryogenesis in plants. Front Plant Sci 6:635. https://doi.org/10.3389/fpls.2015.00635
7. Dodeman VL, Ducreux G, Kreis M (1997) Zygotic embryogenesis versus somatic embryogenesis. J Exp Bot 48:1493-1509.
8. Fehér A (2005) Why somatic plant cells start to form embryos? In: Mujib. A.; Šamaj, J. (eds). Somatic embryogenesis. Springer, Berlin, pp 85-101. https://doi.org/10.1007/7089_019
9. Ferreira JCB, Silva-Cardoso IMA, Meira RO, Scherwinski-Pereira JE (2022) Somatic embryogenesis and plant regeneration from zygotic embryos of the palm tree *Euterpe precatoria* Mart. Plant Cell, Tissue Organ Cult148:667-686. https://doi.org/10.1007/s11240-022-02227-2

10. Freitas EO, Monteiro TR, Nogueira GF, Scherwinski-Pereira JE (2016) Somatic embryogenesis from immature and mature zygotic embryos of the açai palm (*Euterpe oleracea*): Induction of embryogenic cultures, morphoanatomy and its morphological characteristics. Sci Hort 212(14):126-135. http://dx.doi.org/10.1016/j.scienta.2016.09.044
11. Forcat S, Bennett MH, Mansfield JW, Grant MR (2008) A rapid and robust method for simultaneously measuring changes in the phytohormones ABA, JA and SA in plants following biotic and abiotic stress. Plant Methods 4(1):16. https://doi.org/10.1186/1746-4811-4-16
12. Garcia JAA, Corrêa RCG, Barros L, Pereira C, Abreu RMV, Alves MJ, Calhelha RC, Bracht A, Peralta RM, Ferreira ICFR (2019) Chemical composition and biological activities of Juçara (*Euterpe edulis* Martius) fruit by-products, a promising underexploited source of high-added value compounds. J Func Foods 55:325-332. https://doi.org/10.1016/j.jff.2019.02.037
13. Ghosh A, Igamberdiev AU, Debnath SC (2021) Tissue culture-induced DNA methylation in crop plants: a review. Mol Biol Rep 48:823-841. https://doi.org/10.1007/s11033-020-06062-6
14. Guerra MP, Handro W (1988) Somatic embryogenesis and plant regeneration in embryo cultures of *Euterpe edulis* Mart. (Palmae). Plant Cell Rep 7(7):550-552. https://doi.org/10.1007/BF00272754
15. Guerra MP, Handro W (1998) Somatic embryogenesis and plant regeneration in different organs of *Euterpe edulis* Mart. (Palmae): Control and structural features. J Plant Res 111(1)65-71. https://doi.org/10.1007/BF02507151
16. Gutmann M, Von Aderkas P, Label P, Lelu M-A (1996) Effects of abscisic acid on somatic embryo maturation of hybrid larch. J Exp Bot47:1905-1917. https://doi.org/10.1093/jxb/47.12.1905
17. Hasan M, Skalicky M, Jahan MS, Hossain M, Anwar Z, Nie ZF, Alabdallah NM, Brestic M, Hejnak V, Fang XW (2021) Spermine: Its emerging role in regulating dry stress responses in plants. Cells 10(261)215. https://doi.org/10.3390/cells10020261
18. Hildebrandt TM, Nesi AN, Araújo WL, Braun HP (2015) Amino acid catabolism in plants. Mol Plant 8(11): 1563-1579. https://doi.org/10.1016/j.molp.2015.09.005
19. Huang XL, Li XJ, Li Y, Huang LZ (2008) The effect of AOA on ethylene and polyamine metabolism during early phases of somatic embryogenesis in *Medicago sativa*. Physiol Plant113(3) 424-429. DOI: https://doi.org/10.1034/j.1399-3054.2001.1130317.x
20. Ikeuchi M, Ogawa Y, Iwase A, Sugimoto K (2016) Plant regeneration: cellular origins and molecular mechanisms. Development 143:1442-1451. https://doi.org/10.1242/dev.134668
21. Isah T (2016) Induction of somatic embryogenesis in woody plants. Acta Physiol Plant 38(118) 1-22. https://doi.org/10.1007/s11738-016-2134-6
22. Kępczyńska E, Ruduś I, Kępczyński J (2009) Endogenous ethylene in indirect somatic embryogenesis of *Medicago sativa* L. Plant Growth Regul 59(1):63-73. https://doi.org/10.1007/s10725-009-9388-6
23. Ledo AS, Lameira AO, Benbadis AK, Menezes IC, Oliveira MSP, Medeiros Filho S (2002) Somatic embryogenesis from zygotic embryos of *Euterpe oleracea* Mart. Rev Bras Frut 24(3)601-603. https://doi.org/10.1590/S0100-29452002000300004

24. Murashige T, Skoog F (1962) A revised medium for rapid growth and bioassays with tobacco tissue cultures. Physiol Plant 15:473-497. https://doi.org/10.1111/j.1399-3054.1962.tb08052.x
25. Nandy S, Das T, Tudu CK, Mishra T, Ghorai M, Gadekar VS, Anand U, Kumar M, Behl T, Shaikh NK, Jha NK, Shekhawat MS, Pandey DK, Dwivedi PR, Dey A (2022) Unravelling the multi-faceted regulatory role of polyamines in plant biotechnology, transgenics and secondary metabolomics. Appl Microbiol Biotechnol106:905-929. https://doi.org/10.1007/s00253-021-11748-3
26. Oliveira LB, Mello T, Araujo CP, Oliveira JPB, Ferreira A, Zanardo EC, Vieira L M, Otoni WC, Alexandre RS, Carvalho VS (2022) Morphoanotomical aspects of auxinic herbicides-induced somatic embryogenesis in *Euterpe edulis* Martius - a symbol and threatened species of the Atlantic Forest. Sci Hort 299:111051. https://doi.org/10.1016/j.scienta.2022.111051
27. Polesi LG, Fraga HPF, Goeten D, Back FP, Oliveira EM, Steiner N, Guerra MP (2022) Morphohistological and biochemical features of the Guadua chacoensis (Bambusoideae; Poaceae) somatic embryogenesis. Plant Cell, Tissue Organ Cult 148(3):479-499. https://doi.org/10.1007/s11240-021-02199-9
28. O'Brien TP, Mccully ME (1981) The study of plant structure principles and select methods. Melbourne: Termarcarphi Pty, 45p.
29. R Core Team (2020) R: a language and environment for statistical computing. Vienna: R Foundation for Statistical Computing. Available in: <https://www.rproject.org/>. Accessed on: 10 Feb. 2020.
30. Rocha DI, Pinto DLP, Vieira LM, Tanaka FAO, Dornelas MC, Otoni WC (2016) Cellular and molecular changes associated with competence acquisition during passion fruit somatic embryogenesis: ultrastructural characterization and analysis of SERK gene expression. Protoplasma 253(2):595-609. https://doi.org/10.1007/s00709-015-0837-y
31. Rodriguez-Sanz H, Manzanera JA, Solis MT, Gomez-Garay A, Pintos B, Risueno MC, Testillano PS (2014) Early markers are present in both embryogenesis pathways from microspores and immature zygotic embryos in cork oak, *Quercus suber* L. BMC Plant Biol 14(224) 1-18. https://doi.org/10.1186/s12870-014-0224-4
32. Silva-Cardoso IMA, Gomes ACMM, Scherwinski-Pereira JE (2022) Cellular responses of oil palm genotypes during somatic embryogenesis involve participation of procambial cells, DNA demethylation, and auxin accumulation. Plant Cell Rep 41:1875-1893. https://doi.org/10.1007/s00299-022-02898-3
33. Scherwinski-Pereira JE, Guedes RS, Silva RA, Fermino JR, Luis ZG, Freitas EO (2012) Somatic embryogenesis and plant regeneration in açaí palm (*Euterpe oleracea*). Plant Cell, Tissue Organ Cult 109(3):501-508. https://doi.org/10.1007/s11240-012-0115-z
34. Schulz M, Borges GDSC, Gonzaga LV, Costa ACO, Fett R (2016) Juçara fruit (*Euterpe edulis* Mart.): Sustainable exploitation of a source of bioactive compounds. Food Res Int 89:14-26. https://doi.org/10.1016/j.foodres.2016.07.027
35. Silva-Cardoso IMA, Meira FS, Gomes ACMM, Scherwinski-Pereira JE (2020) Histology, histochemistry and ultrastructure of pre-embryogenic cells determined for direct somatic

embryogenesis in the palm tree *Syagrus oleracea*. Physiol Plant 168(4):845-875. https://doi.org/10.1111/ppl.13026

36. Stein VC, Paiva R, Vargas DP, Soares FP, Alves E, Nogueira GF (2010) Ultrastructural calli analysis of *Inga vera* Willd. subsp. *affinis* (DC.) T.D. Penn. Rev Árv 34(5):789-796. https://doi.org/10.1590/S0100-67622010000500004
37. Toumi I, Moschou PN, Paschalidis KA, Bouamama B, Salem-Fnayou AB, Ghorbel AW, Mliki A, Roubelakis-Angelakis KA (2010) Abscisic acid signals reorientation of polyamine metabolism to orchestrate stress responses via the polyamine exodus pathway in grapevine. J Plant Physiol 167:519-525. https://doi.org/10.1016/j.jplph.2009.10.022
38. Valledor L, Hasbún R, Meijón M, Rodríguez JL, Santamaría E, Viejo M, Berdasco M, Feito I, Fraga MF, Cañal MJ, Rodríguez R (2007) Involvement of DNA methylation in tree development and micropropagation. Plant Cell, Tissue Organ Cult 91:75-86. https://doi.org/10.1007/s11240-007-9262-z
39. Yang SF, Hoffman NE (1984) Ethylene biosynthesis and its regulation in higher plants. Ann Rev Plant Physiol35:155-189. https://doi.org/10.1146/annurev.pp.35.060184.001103

Figures

(a)

Variables	X̄	Detour (±)
FFM (g)	1.69	0.07
FDM (g)	0.55	0.02
SWC (%)	67.36	1.18
AD (mm)	13.94	0.06
V (cm³)	1.45	0.06
G (%)	100.0	0.00
GSI	2.20	0.04
AGT (d)	11.71	0.20
FrG	0.10	0.00

(b)

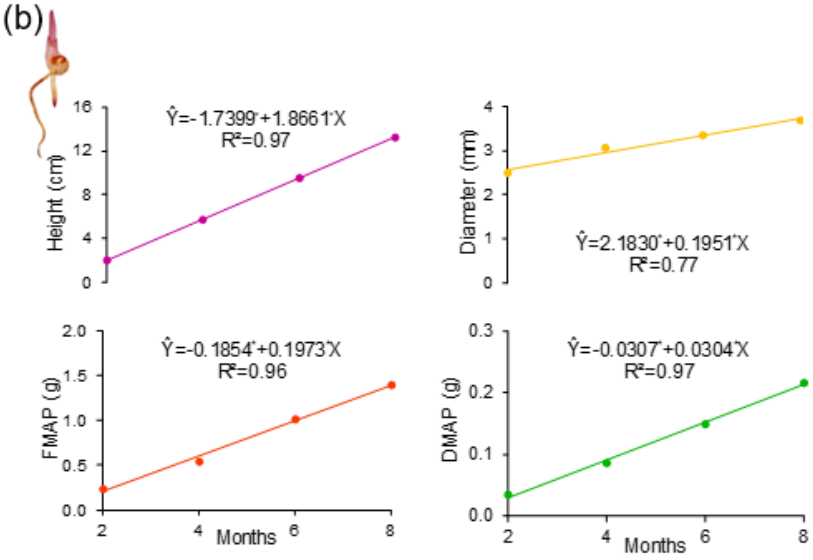

Figure 1

Grwoth and germination parameters of (**a**) seeds and (**b**) seedlings of *E. edulis* with 2, 4, 6, and 8 months of age. FFM, fresh fruit mass; FDM, fruit dry mass; SWC, seed water content; AD, average diameter; V, fruit volume; G, germination; GSI, germination speed index; AGT, average germination time; FrG, relative frequency of germination; FMAP, fresh mass of aerial part; and DMAP, dry mass of aerial part. *Statistically significant coefficient at 5% (*t*-test)

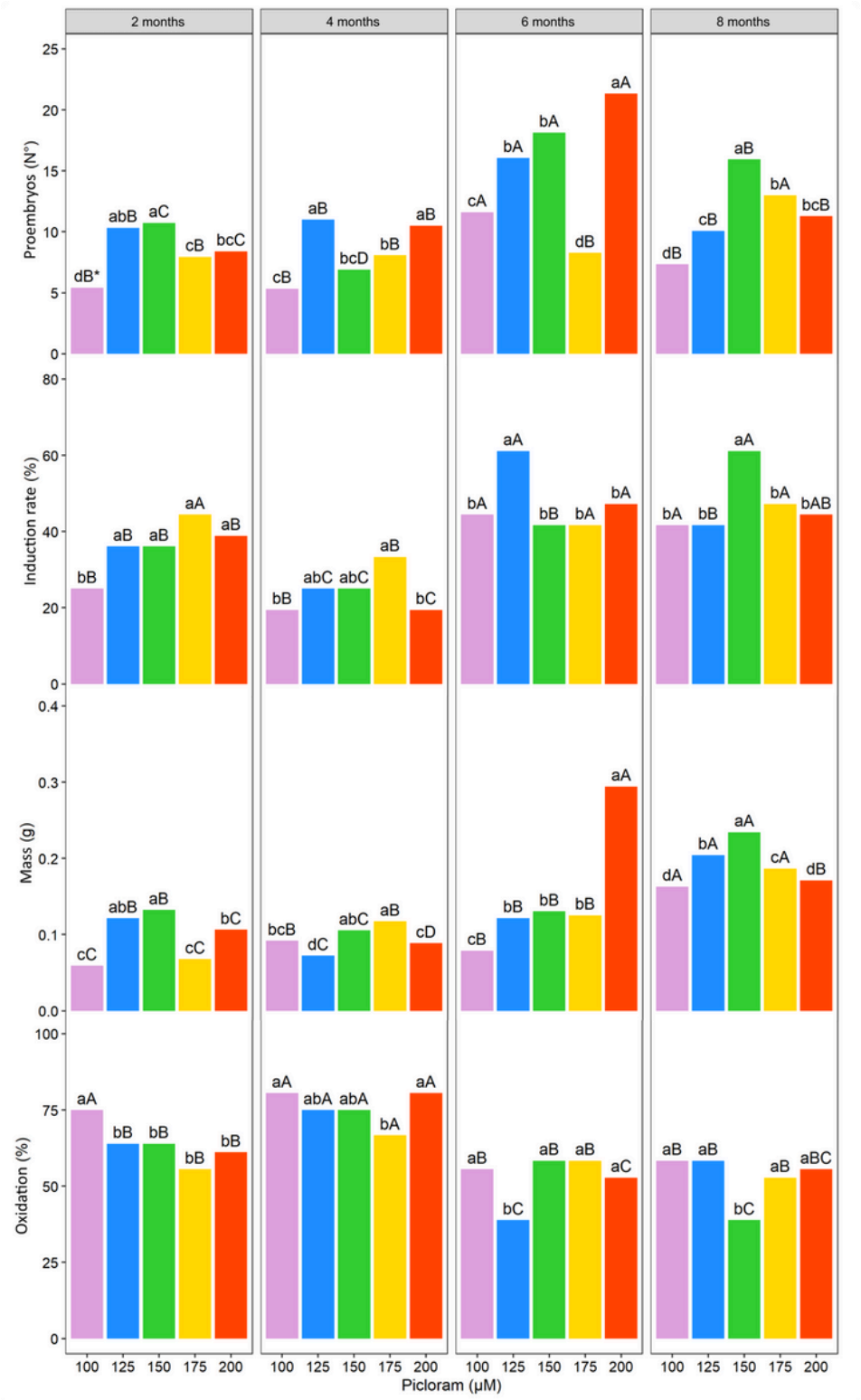

Figure 2

Induction of somatic embryogenesis in *E. edulis* explants of different ages and at different picloram concentrations. (**a**) Number of proembryos, (**b**) induction rate, (**c**) explant mass, and (**d**) oxidation. [1]Averages not followed by the same lowercase letter (between concentrations at the same age) and capital letter (between ages at the same concentration), differ by Tukey's test ($p < 0.05$). Bar: 1 cm

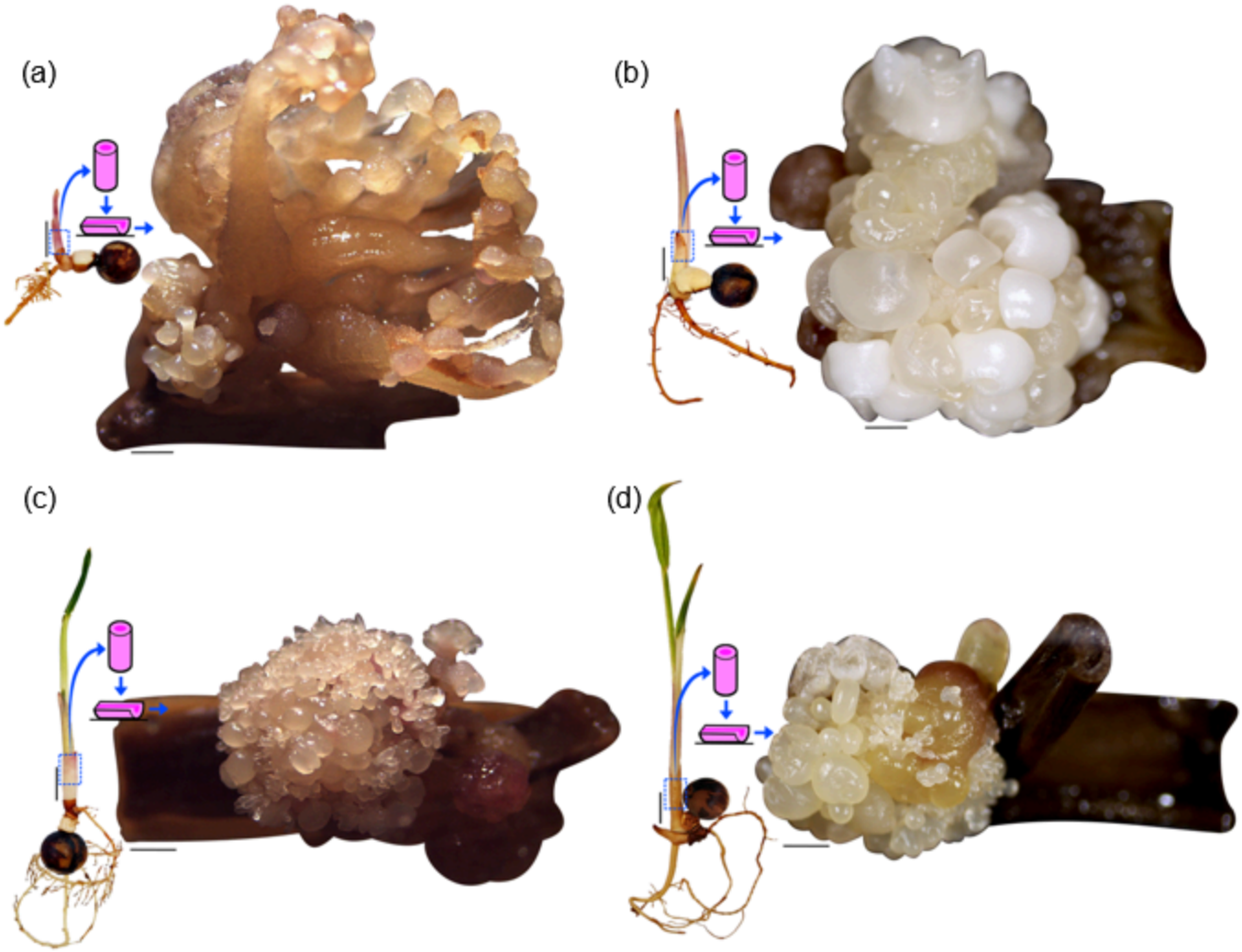

Figure 3

Induction of somatic embryogenesis with stem segments of *E. edulis* seedlings at different ages, after treatment with 150 μM picloram: (**a**) 2 months, (**b**) 4 months, (**c**) 6 months, and (**d**) 8 months. Bar: seedlings 1 cm, explants 1 mm

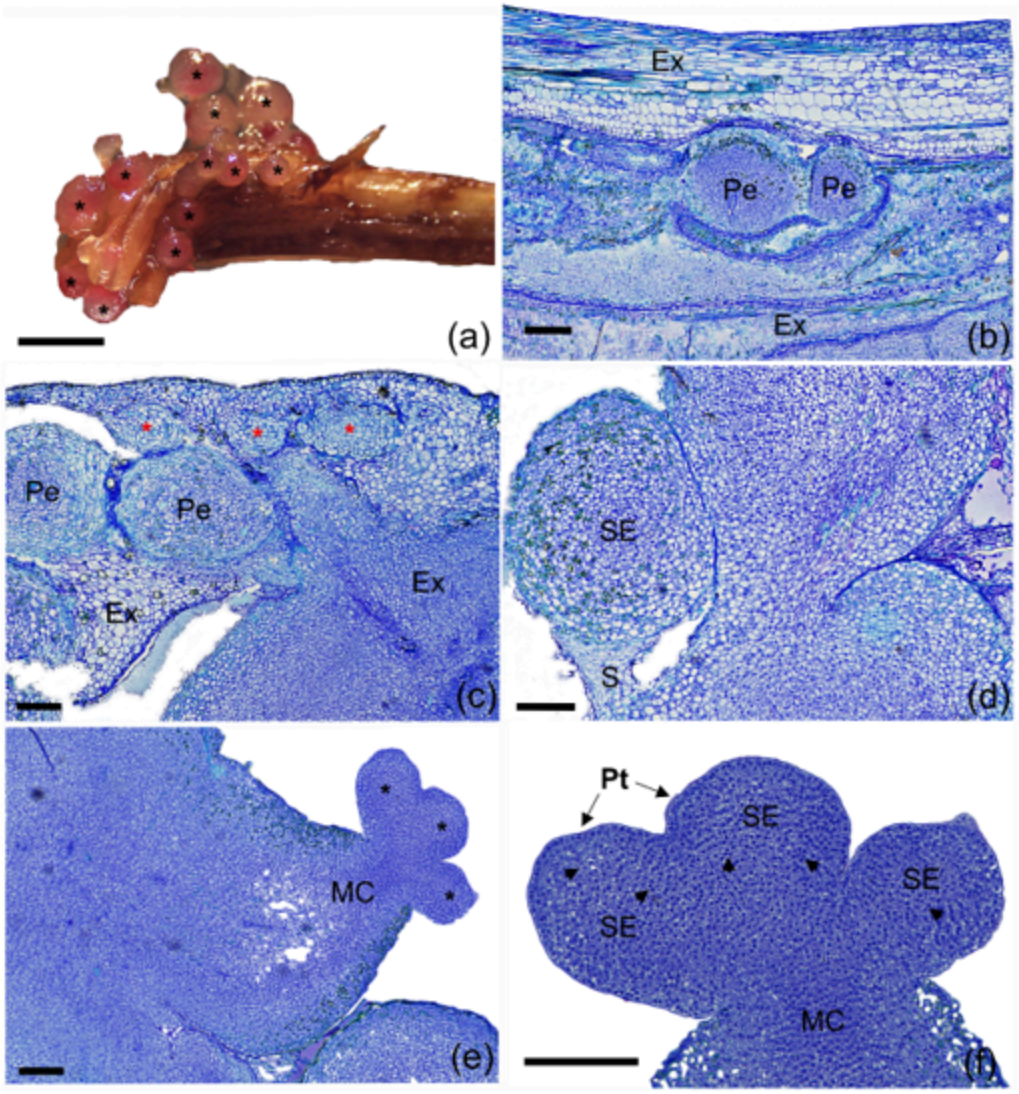

Figure 4

Somatic embryogenesis in the stem of 6-month-old *E. edulis* seedlings induced with picloram. (**a**) Macroscopic image, highlighting the formation of somatic embryos (*). (**b–f**) histological sections showing (**b**) somatic proembryos (Pe) inside the explant (Ex); (**c**) somatic embryos protruding from the explant (Pe, red *); (**d**) formation of globular somatic (SE) embryo with suspensor (S); (**e**) globular somatic embryo without suspensor, originating from meristematic cells (MC); and (**f**) subepidermal cells dividing in different planes forming clusters of cells in anticlinal and periclinal division (arrows) underneath the protoderm (Pt). Bar: 2000 μm (a), 400 μm (b–f)

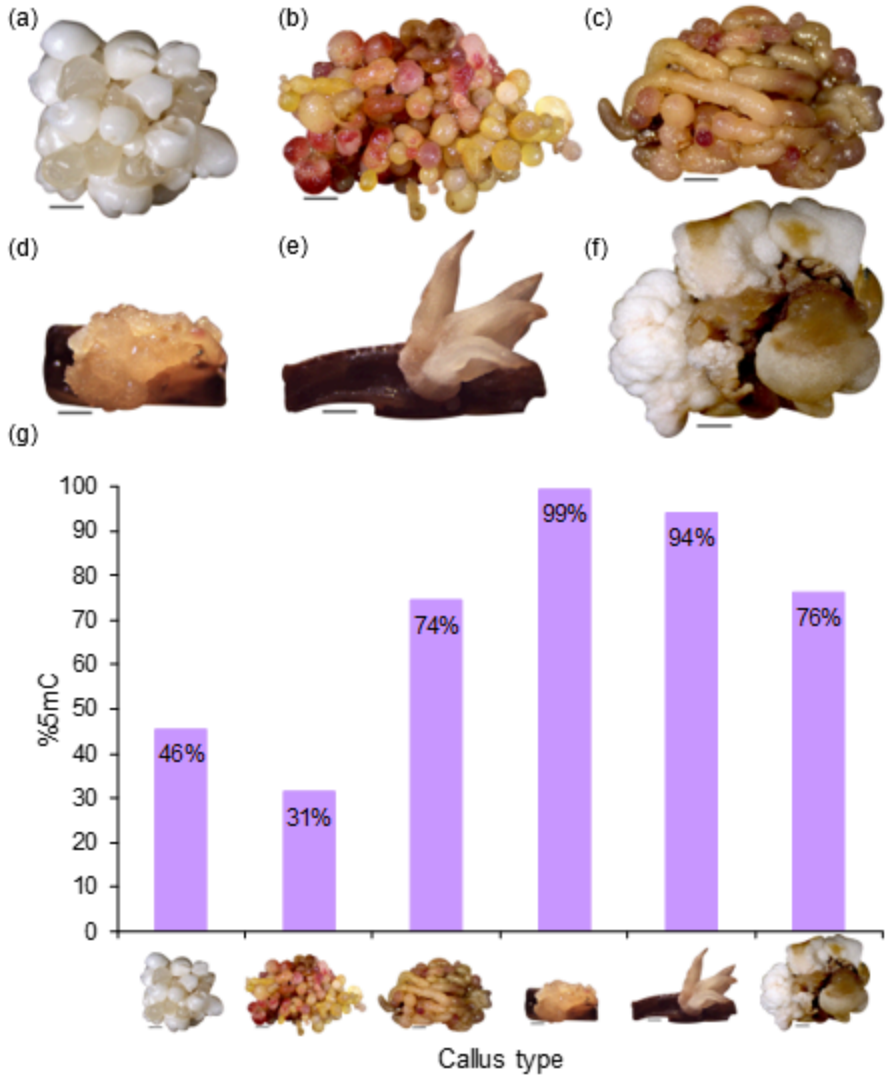

Figure 5

Different structures produced during embryogenic induction of stem segments from 6-month-old seedlings of *E. edulis*. (**a**) Embryogenic structure with white somatic embryos; (**b**) embryogenic structure with yellow somatic embryos; (**c**) elongated embryogenic and non-embryogenic structures; (**d**) non-embryogenic, yellow compact callus; (**e**) leafy structures; (**f**) white callus. (**g**) Global DNA methylation (%5mC) in each callus type. Bar: 2000 µm

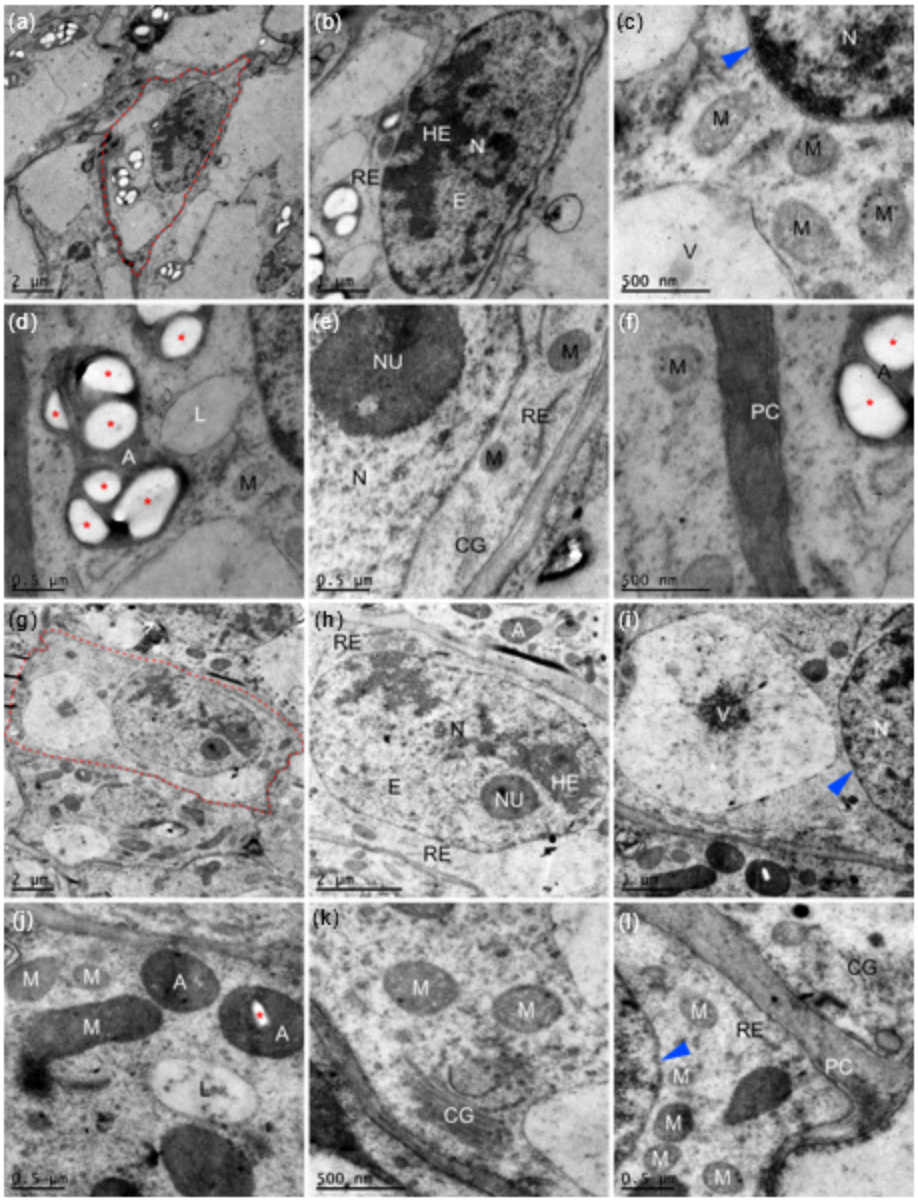

Figure 6

Ultrastructures visible within embryogenic tissue induced from stem segments obtained from (**a–f**) 2-month-old or (**g–l**) 8-month-old seedlings of *E. edulis* treated with 150 µM picloram. (**a, g**) Cell contour (dashed red line). (**b, h**) Nucleus (N), heterochromatin (HE), euchromatin (E), and endoplasmic reticulum (ER). (**c, i**) Nucleus, nuclear membrane (blue arrow), mitochondria (M), and vacuole (V). (**d, j**) Amyloplasts (A), starch granules (red *), and lysosome (L). (**e, k**) Nucleolus (NU) and nucleus with endoplasmic reticulum, mitochondria, and Golgi complex (GC) around it. (**f, l**) Cell wall (PC)

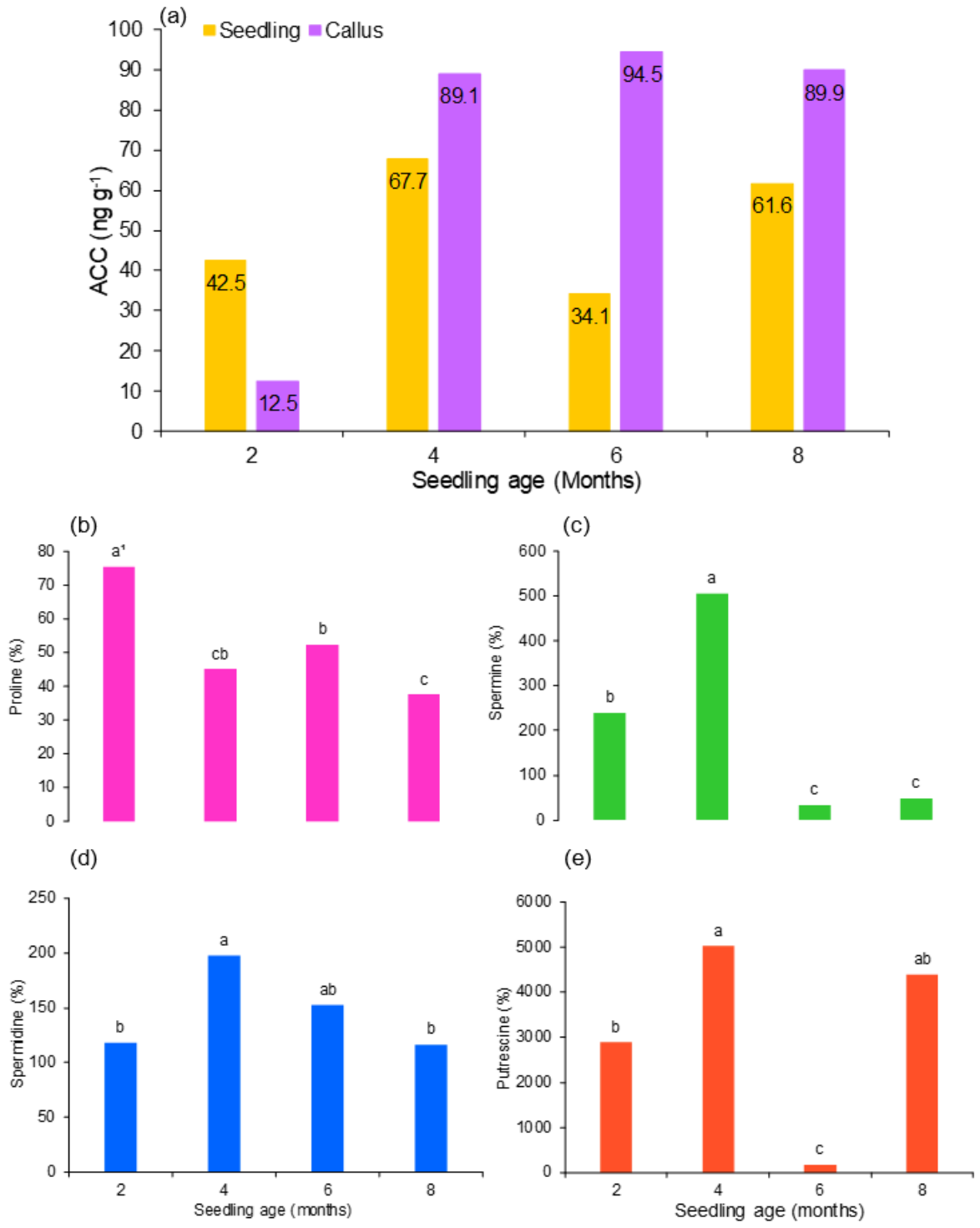

Figure 7

Concentration of various metabolites in aerial parts and calli of *E. edulis* in relation to seedling age. (**a**) ACC in the aerial part of seedlings and in the corresponding calli, (**b**) proline, (**c**) spermine, (**d**) spermidine, and (**e**) putrescine. [1]Means followed by the same letter do not differ according to Tukey's test ($p < 0.05$).

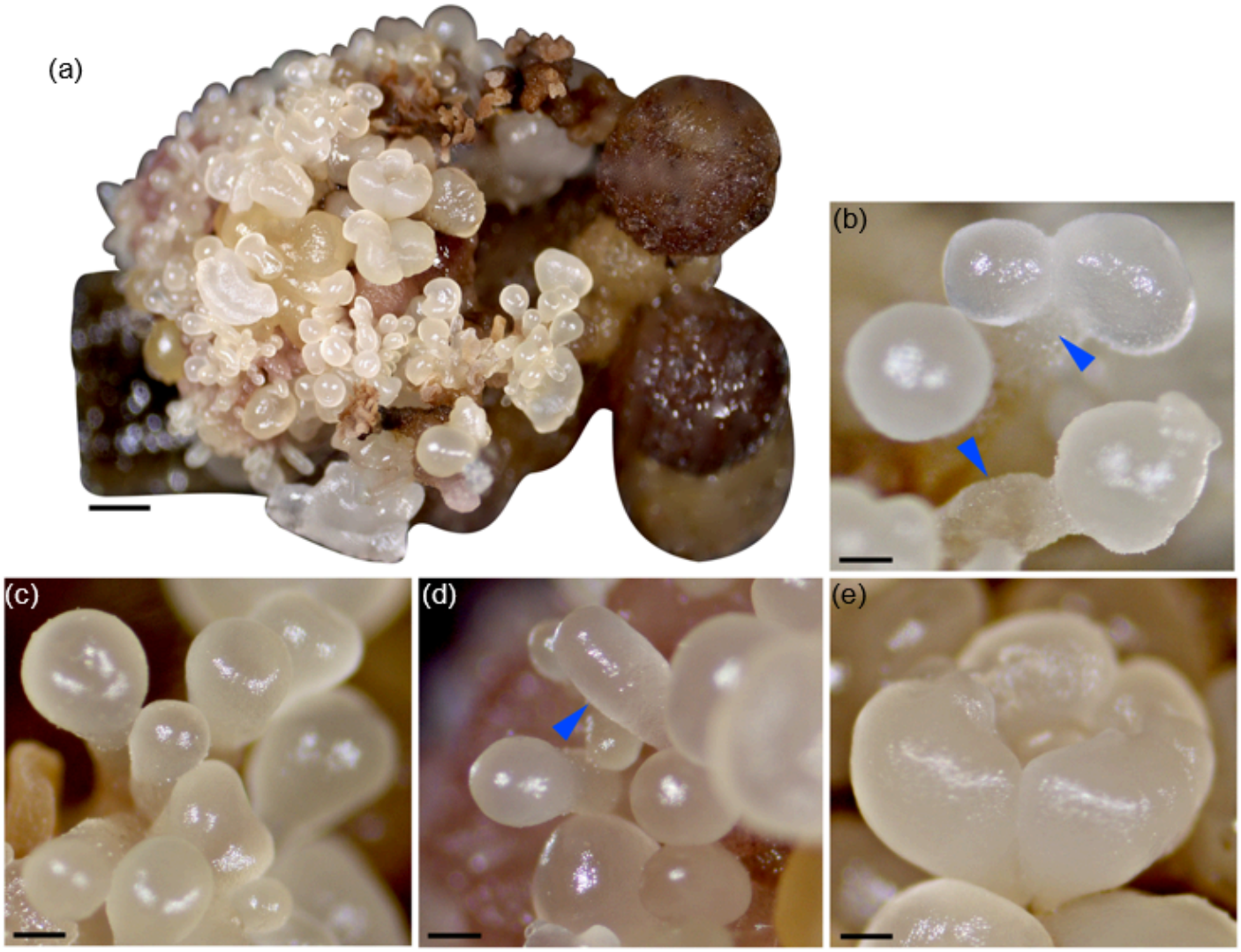

Figure 8

Maturation of somatic embryos from stem segments of 6-month-old seedlings of *E. edulis*, induced with 5 µM abscisic acid. (**a**) Explant showing asynchronous growth, (**b**) globular somatic embryos with suspensor (arrows), (**c**) somatic embryos transitioning to scutellar embryos, (**d**) scutellar somatic embryo (arrow), and (**e**) coleoptilar somatic embryo. Bar: 1 mm (a), 200 µm (b–e)

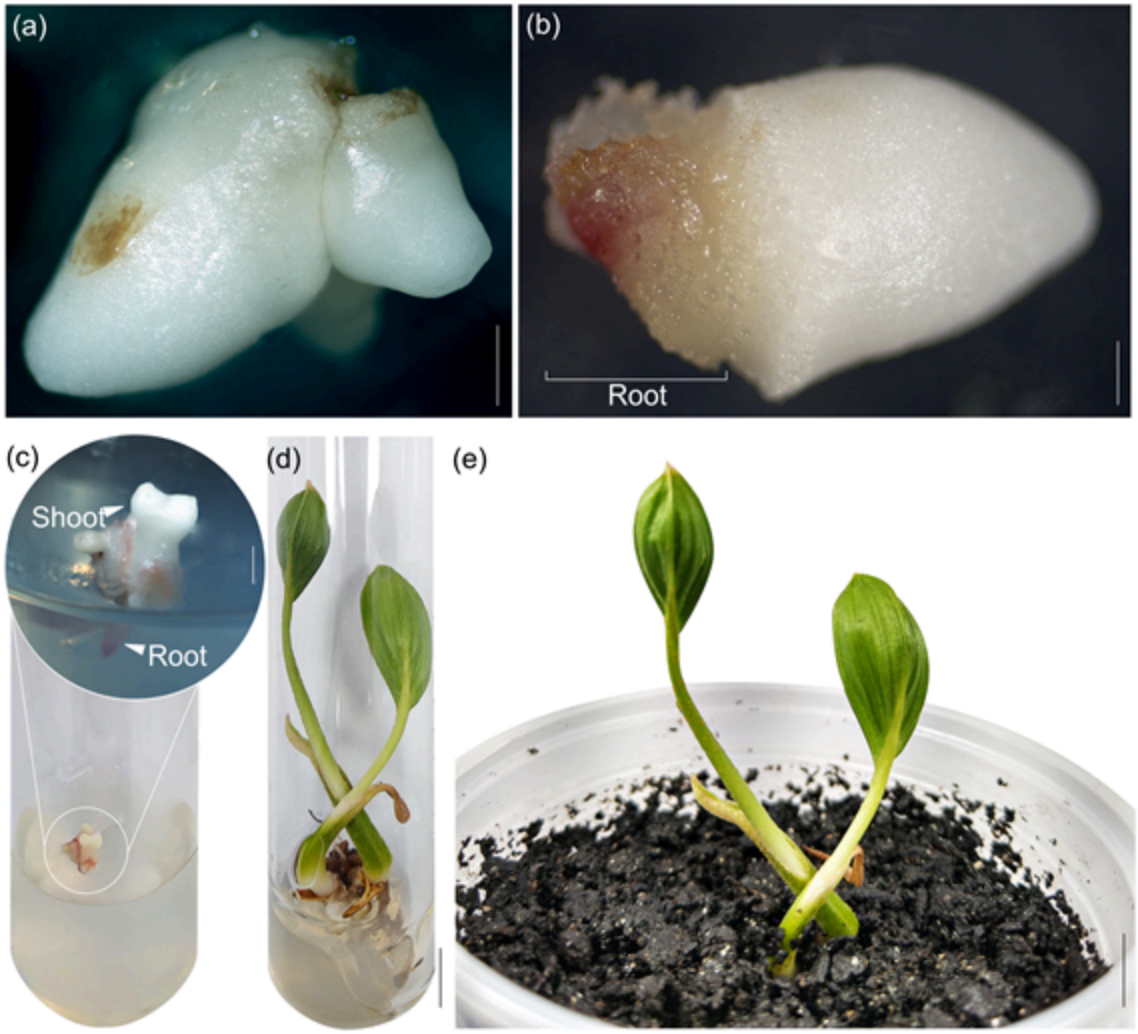

Figure 9

Conversion of somatic embryos into emblings of *E. edulis*. (**a**) Coleoptilary somatic embryo, (**b**) primary root protrusion, (**c**) shoot formation, (**d**) embling, and (**e**) embling acclimatisation. Bar: 500 µm (a, b), 1000 µm (c), 1 cm (d, e).

Supplementary Files

This is a list of supplementary files associated with this preprint. Click to download.

- Protocol.tiff